Open access • Journal Article • DOI:10.1016/J.IJROBP.2016.01.055

First Clinical Investigation of Cone Beam Computed Tomography and Deformable Registration for Adaptive Proton Therapy for Lung Cancer. — Source link

C. Veiga, Guillaume Janssens, Ching Ling Teng, Thomas Baudier ...+11 more authors

Institutions: University College London, Université catholique de Louvain, University of Pennsylvania

Published on: 01 May 2016 - International Journal of Radiation Oncology Biology Physics (Elsevier)

Topics: Cone beam computed tomography

Accepted Manuscript

First clinical investigation of CBCT and deformable registration for adaptive proton therapy of lung cancer

Catarina Veiga, MSc, Guillaume Janssens, PhD, Ching-Ling Teng, PhD, Thomas Baudier, BSc, Lucian Hotoiu, PhD, Jamie R. McClelland, PhD, Gary Royle, PhD, Liyong Lin, PhD, Lingshu Yin, PhD, James Metz, PhD, Timothy D. Solberg, PhD, Zelig Tochner, MD, Charles B. Simone, II, MD, James McDonough, PhD, Boon-Keng Kevin Teo, PhD

PII: S0360-3016(16)00108-5

DOI: 10.1016/j.ijrobp.2016.01.055

Reference: ROB 23414

To appear in: *International Journal of Radiation Oncology • Biology • Physics*

Received Date: 30 September 2015

Revised Date: 26 January 2016

Accepted Date: 28 January 2016

Please cite this article as: Veiga C, Janssens G, Teng C-L, Baudier T, Hotoiu L, McClelland JR, Royle G, Lin L, Yin L, Metz J, Solberg TD, Tochner Z, Simone II CB, McDonough J, Teo B-KK, First clinical investigation of CBCT and deformable registration for adaptive proton therapy of lung cancer, *International Journal of Radiation Oncology • Biology • Physics* (2016), doi: 10.1016/j.ijrobp.2016.01.055.

TITLE PAGE

Title: First clinical investigation of CBCT and deformable registration for adaptive proton therapy of lung cancer
Running title: Adaptive proton therapy workflow using CBCT

Authors:
Catarina Veiga[1], MSc; Guillaume Janssens[2], PhD; Ching-Ling Teng[3], PhD; Thomas Baudier[4], BSc; Lucian Hotoiu[4]; PhD; Jamie R. McClelland[5], PhD; Gary Royle[1], PhD; Liyong Lin[3], PhD; Lingshu Yin[3], PhD; James Metz, PhD[3]; Timothy D Solberg[3], PhD; Zelig Tochner[3], MD; Charles B. Simone, II[3], MD; James McDonough[3], PhD; Boon-Keng Kevin Teo[3], PhD

Affiliations:
[1]Proton and Advanced RadioTherapy Group, Department of Medical Physics & Biomedical Engineering, University College London, London, UK
[2]Ion Beam Applications SA, Louvain-la-Neuve, Belgium
[3]Department of Radiation Oncology, University of Pennsylvania, Philadelphia, PA, United States
[4]iMagX Project, ICTEAM Institute, Université Catholique de Louvain, Louvain-la-Neuve, Belgium
[5]Centre for Medical Image Computing, Department of Medical Physics & Biomedical Engineering, University College London, London, UK

Conflict of interest: Dr. McDonough reports grants from Department of Defense, during the conduct of the study; Dr. Metz reports other from IBA, outside the submitted work.

Acknowledgments: C. V. was funded by Fundação para a Ciência e a Tecnologia (FCT) grant SFRH/BD/76169/2011, co-financed by FSE, POPH/QREN and EU. J.M. was supported by the EPSRC Intelligent Imaging Program Grant EP/H046410/1. This work was supported by the US Army Medical Research and Materiel Command under Contract Agreement no DAMD17-W81XWH-04-2-0022. Opinions, interpretations, conclusions and recommendations are those of the author and are not necessarily endorsed by the US Army.

Corresponding author:
Boon-Keng Kevin Teo PhD,
3400 Civic Center Boulevard, TRC 2 West
Department of Radiation Oncology
University of Pennsylvania
Philadelphia, PA, 19104

SUMMARY

Accurate patient positioning and routine computed tomography (CT) scans are critical components of proton therapy. Cone-beam CT (CBCT) has recently become available as an alternative to verification CT. This study describes the first clinical investigation of CBCT and deformable registration in adaptive lung proton therapy.

ABSTRACT

Purpose: An adaptive proton therapy workflow using cone-beam computed tomography (CBCT) is proposed. It consists of an online evaluation of a fast range-corrected dose distribution based on a virtual CT (vCT). This may be followed by more accurate offline dose recalculation on the vCT which may trigger a rescan CT (rCT) for replanning.

Methods and Materials: The workflow was tested retrospectively on twenty consecutive lung cancer patients. A diffeomorphic Morphons algorithm was used to generate the lung vCT, by deforming the average planning CT (pCT) onto the CBCT. An additional correction step was applied to account for anatomical modifications that cannot be modeled by deformation alone. A set of clinical indicators for replanning were generated based on water equivalent thickness (WET) and dose statistics, and compared to those obtained on a rCT. The fast dose approximation consisted of warping the initial planned dose onto the vCT based on changes in WET. Potential under/over-ranges were assessed as variation in WET at the target's distal surface.

Results: The range-corrected dose from the vCT reproduced similar clinical indicators as the rCT. The workflow performed well under different clinical scenarios: atelectasis, lung reinflation and different types of tumor response. Between vCT and rCT, we found a difference in the measured 95% percentile of the over-ranges distribution of 3.4±2.7mm. The limitations of the technique consisted of inherent uncertainties of deformable registration and drawbacks of CBCT imaging. The correction step was adequate when gross errors occurred but could not recover subtle anatomical or density changes in tumors with complex topology.

Conclusions: A proton therapy workflow based on CBCT provided similar clinical indicators as rCT on lung patients with considerable anatomical changes.

1. INTRODUCTION

Lung cancer is the leading cause of cancer-related death in the United States and worldwide. Modern radiotherapy techniques allow dose escalation[1,2] and reduced injuries to normal tissues[3-6]. Proton therapy offers better dose localization than that achieved by conventional photon therapy.[7-11] Proton dose distribution, however, is highly sensitive to changes in patient geometry, especially in the lungs.[12] For example, interfractional tumor enlargement or development of atelectasis increase density along the beam path and shorten beam penetration. The under-ranging can potentially reduce target coverage. Conversely, tumor regression reduces density along the beam path and increases beam penetration. The over-ranging may result in unplanned dose to otherwise spared organs distal to the tumor volume. Therefore, accurate patient positioning and regular evaluation computed tomography (CT) scans are critical components of proton therapy.[13] Replanning will be required if the new dose distribution based on evaluation CTs compromises target coverage and/or exceeds tissue tolerance.

Volumetric imaging afforded by on-board cone-beam CT (CBCT) is an alternative to routine CT imaging and may play an important role in adaptive radiation therapy (ART). The advantages of on-board CBCT are threefold: (1) it offers highly accurate patient positioning in three dimensions;[14,15] (2) it enables daily monitoring of the patient in the treatment position; and (3) and it facilitates rapid assessment of the "dose of the day".[16-18]

We propose an ART workflow using on-board CBCT where replanning is triggered after three decision-points (Fig. 1). First, a fast range-corrected dose distribution based on water equivalent thickness (WET) is calculated on a virtual CT (vCT) derived from the CBCT.[19] When significant dosimetric changes are observed, treatment may continue if normal tissue dose limits are not exceeded and after consultation with a physician. However, an offline review is triggered for a full dose recalculation on the vCT. If the dosimetric impact is still evaluated as significant, a rescan CT (rCT) is scheduled. If dosimetric changes are confirmed on the rCT, a replan is triggered. We retrospectively evaluated this workflow for twenty consecutive lung cancer patients summarizing common radiation-induced changes in the lung and critically assessed the workflow. The rCT was used as the gold-standard to gauge the accuracy of the vCT. To our knowledge, this study is the first clinical investigation of CBCT in adaptive lung proton therapy.

2. METHODS AND MATERIALS

2.1. Patient selection and data acquisition

Data from twenty consecutive patients treated for lung malignancies were included in this retrospective study. All patients underwent passive scattering proton therapy (PSPT) using two treatment fields with a median dose of 66.3Gy[CGE] (range:40-66.6Gy[CGE]) in a median of 1.8Gy/fraction (range:1.5-4Gy/fraction). The patient cohort included a variety of tumor sizes, locations and anatomical changes that occurred throughout the treatment course (Table 1). The imaging protocol consisted of a 4D PET/CT for treatment planning, CBCT and rescan 4D CT acquired in treatment position for verification during the course of treatment. The proton-gantry mounted CBCT system (Ion Beam Applications SA, Ottignies-Louvain-la-Neuve, BE) has a source-to-axis distance of 288.4cm, detector-to-axis distance of 58.6cm and a maximum field-of-view (FoV) of 34cm; the images were acquired in half-scan mode at 110kVp and 1142mAs. The CBCTs were reconstructed with a resolution of $1.33\times1.33\times2.5mm^3$ using the open-source Reconstruction Toolkit (RTK).[20] The average phase of the 4D CT was used for dose calculations. One pair of CBCT and rCT at mid-treatment was selected for evaluation for each patient. The chosen rCT and CBCT scans were acquired on the same day for 17 patients; for 3 they were acquired within 2 days of each other.

2.2. Virtual CT and image correction

The CBCT was rigidly aligned to the planning CT (pCT) and the diffeomorphic Morphons deformable image registration (DIR) algorithm available in the open-source REGGUI package was subsequently applied to register the pCT to the CBCT.[21] This method was previously validated for head and neck cancer patients.[16,17]

Some anatomical changes in the thorax cannot be modeled by deformation alone. The situations are diverse, but include changes within the lung (such as atelectasis and pleural effusion) and different tumor responses to treatment (such as regression of infiltrating tumors and erosion[22]). Therefore, a semi-automatic correction step was applied to the vCT for these anatomical modifications. This step consists of a watershed-cuts algorithm[23,24] combined with an exclusive OR logical operator and a classifier[25,26] to identify regions showing significant intensity mismatch between vCT and CBCT. When appropriate, the vCT intensities were replaced by the bulk value of lung or tissue based on thresholding of the CBCT intensities. This algorithm was validated in-house[27]; technical details of the implementation can be found as supplementary material.

2.3. Clinical indicators: WET and dose warping

A complementary set of clinical indicators, based on WET and dose, that support the replanning decision-making, were used to estimate the impact of anatomical changes on the treatment objectives.

Variation in WET on the distal surface of the target is a good surrogate for potential under/over-ranges. Changes in range were estimated by computing the difference between the WET from the pCT and vCT (i.e. $WET_{pCT}>WET_{vCT}$ corresponds to over-ranging and $WET_{pCT}<WET_{vCT}$ to under-ranging). In PSPT compensator smearing is used to ensure target coverage in presence of errors in patient positioning and motion.[28] Therefore, potential under-ranges are partially taken into account by the compensator; thus, for under-ranges a morphological dilation using the same radius as the compensator is applied on the pCT-based WET map before computing the difference with the vCT-based WET map to identify under-ranges not accounted for in smearing. Quantitative measurements of the 2D WET difference maps at the PTV distal surface (per beam) for the pCT and vCT were calculated as clinical indicators, which include the percentage of pixels with under/over-ranges larger than 3mm ($WET_{under>3mm}$/$WET_{over>3mm}$) and the 95% percentile of the under/over-range distribution ($WET_{under-95\%}$/$WET_{over-95\%}$).

Complementary to the WET analysis, it is necessary to evaluate the dosimetric impact of under/over-ranging, particularly for OAR. Online dose review requires a fast dose recalculation tool; thus we validated in-house a fast range-corrected dose approximation method[29] by warping the original dose onto the vCT based on changes in the 3D WET maps between the vCT and pCT. Doses were recalculated using Eclipse version 11.0 (Varian Medical Systems, Palo Alto, CA). The following abbreviations are used to identify the different doses: pCT dose (D_{pCT}), vCT warped dose ($D_{vCT\text{-}WET}$), vCT recalculated dose (D_{vCT}) and rCT recalculated dose (D_{rCT}). DVHs and dosimetric statistics representative of target coverage and OAR tolerances used in-house to trigger replanning were chosen as dose indicators. These were for PTV and iCTV the $V_{95\%}$ and $V_{99\%}$, respectively, with a threshold of 3% change in the rCT. For OARs the dose tolerances used were: for heart, D_{max}=72Gy, $V_{45Gy}<35\%$ and $V_{30Gy}<50\%$; for esophagus, D_{max}=70Gy and $V_{55Gy}<30\%$; for cord (and cord+5mm), D_{max}=50Gy(65Gy); and for brachialplexus, D_{max}=66Gy. The iCTV/PTV contours were rigidly propagated while the OARs were propagated using DIR.

3. RESULTS

3.1 Case studies of different anatomical changes

3.1.1 Lung changes

Atelectasis is the collapse of lung that is sometimes reversible. PT#1 developed partial atelectasis at the upper left lobe during week two (Fig. 2) resulting in increased WET along the beam paths and subsequent under-ranging ($WET_{under-95\%}$=10.4/12.3mm for LPO_1/LPO_2 field). Tumor coverage was compromised and a higher dose was delivered to the esophagus (D_{max} from 50Gy to 71/71/68Gy for

$D_{vCT\text{-}WET}/D_{vCT}/D_{rCT}$) which triggered immediate replanning. The vCT predicted similar dosimetric indicators as the rCT.

When tumors regress, the previously blocked airway can reopen and reinflate the collapsed lung (PT#3, Fig. 3). Lung reinflation reduced the WET along the beam path, and caused beam over-ranging ($WET_{over\text{-}95\%}$=41.4/44.1mm for RPO/PA field). The change in dose distribution compromised tumor coverage (iCTV $\Delta V_{99\%}$=-27/-27/-13% for $D_{vCT\text{-}WET}/D_{vCT}/D_{rCT}$), which triggered replanning. The predicted loss of coverage was higher in the vCT than in rCT, which can be attributed to the partial truncation of the CBCT at the beam entrance (see section 3.1.3).

3.1.2: Tumor changes

Different tumor response scenarios were identified and detailed below.

Infiltrating tumors

For PT#14, the GTV decreased from 4.1 to 2.7cm in diameter after four weeks of treatment (Fig. 3). The uncorrected vCT resulted in DIR errors of the lung tissue between the tumor and chest wall. After applying the correction algorithm, the clinical indicators were nearly identical between vCT and rCT (iCTV $\Delta V_{99\%}$=-5/-7/-6% for $D_{vCT\text{-}WET}/D_{vCT}/D_{rCT}$).

Tumor regression

When tumors regress, the topological changes may not be handled by DIR alone. In PT#2 a 22.3mm cavity appeared within the original tumor volume (Fig. 2). Its size and location were accurately identified and accounted for by the vCT correction step. The reduction in WET along the beam path resulted in beam over-ranging to the heart ($WET_{over\text{-}95\%}$=24.6/25.2mm for RPO_1/RPO_2 field, Figs. 4 and 5). Dosimetric indicators between vCT and rCT were similar (Fig. 4), i.e., decreased iCTV coverage (iCTV $\Delta V_{99\%}$=-7/-6/-8% at $D_{vCT\text{-}WET}/D_{vCT}/D_{rCT}$), and increased dose to the cord (D_{max} from 45 to 52/52/49Gy for $D_{vCT\text{-}WET}/D_{vCT}/D_{rCT}$) and the heart ($V_{45Gy}$ from 25% to 31/31/35% for $D_{vCT\text{-}WET}/D_{vCT}/D_{rCT}$).

Changes in tumor density

PT#20 had both regression and changes in tumor density; the average intensity of the GTV decreased from 30 to -110HU between pCT/vCT and rCT, corresponding to a local WET variation of approximately 7mm. The vCT retained the HUs from the pCT and underestimated the change in

proton range, i.e., $WET_{over>3mm}$=27.0/40.7% for vCT/rCT (RPO_1 field). Regardless of the differences in WET between the vCT and rCT, identical reduction in dose coverage was detected in the DVHs.

Moderate shrinkage/enlargement

Moderate tumor regression was here defined as a visually apparent change in tumor volume less than 25% of its original GTV. An example is PT#11, who has focal shrinkage resulting in modest beam over-ranging ($WET_{over-95\%}$=8.5/7.5mm for AP/RPO field), and an increase in dose to the cord (D_{max} from 30 to 36/37/37Gy for $D_{vCT-WET}/D_{vCT}/D_{rCT}$). PT#16 was the only case of tumor enlargement during radiation treatment; the diameter increased ~5mm along the beam path. Because of the complex organ geometry at the mediastinum, both beam under/over-ranging were observed (i.e., $WET_{under-95\%}$=1.1mm and $WET_{over-95\%}$=3.6mm for RPO field), resulting in increased dose to the cord (D_{max} from 35 to 46/47/40Gy for $D_{vCT-WET}/D_{vCT}/D_{rCT}$), and a right shift of iCTV/PTV DVH curves. In these two cases the vCT and rCT offered similar clinical indicators with DIR alone.

3.1.3: Other factors affecting clinical indicators

In addition to DIR errors, setup variations and differences in the respiratory pattern between CBCT and rCT scans can result in differences between $D_{vCT-WET}/D_{vCT}$ and D_{rCT}. This implies that different clinical indicators are being extracted, and can, therefore, create false positive/negative triggers for offline review. Our online workflow was less robust for patients in whom the magnitude of dose differences arising from setup variations was comparable to those arising from internal anatomical change. For PT#13, tumor shrinkage was well recovered by DIR; however the position of the main bronchi was shifted superiorly in rCT in comparison to the CBCT (Fig. 3). The movement of the main airway cause different predictions of target coverage (iCTV $\Delta V_{99\%}$=+3/+1/-4% for $D_{vCT-WET}/D_{vCT}/D_{rCT}$). WET difference maps were also affected: the magnitude of $WET_{over-95\%}$ was small but the 2D WET maps gave different indicators ($WET_{over>3mm}$ was 18.8/46.6% for vCT/rCT for PT#19 RPO field, see Fig. 5). Clinically, none of these patients required replanning as the dosimetric changes were generally small and the effects averaged out during the course of treatment.

Setup errors should not be confused with systematic drift of tumor position through the treatment course. For PT#5, the primary tumor shifted in the inferior direction, and this was consistent between the CBCT and rCT. DIR accurately described the change in tumor position, but the modest change in WET had minimal effect on target coverage or dose to OAR.

Due to FoV limitations, a minority of CBCTs did not encompass the entire exterior of the patient body at the beam entrance (Fig. 2 and 3). For PT#4, the CBCT truncation resulted in overestimation

of over-ranging of the RPO field ($WET_{over-95\%}$=19.1/11.0mm for rCT/vCT), but the overall changes in range and dosimetry were small (Fig. 4). Nevertheless, uncorrected truncation may in some cases lead to inaccurate clinical indicators (PT#3: iCTV $\Delta V_{99\%}$=-27/-27/-13% and, PT#17: iCTV $\Delta V_{99\%}$ =0/0/-5% for $D_{vCT-WET}/D_{vCT}/D_{rCT}$).

3.2 General results

Eighteen of the twenty patients exhibited tumor regression resulting in over-ranging of the proton beams; two showed considerable under-ranging. These were cases of atelectasis (PT#1) and tumor enlargement (PT#16). For all patients, the average absolute difference in $WET_{over-95\%}$ and $WET_{over>3mm}$ between vCT and rCT were 3.4±2.7mm and 12±12%, respectively. Figure 5 shows examples of WET and WET difference maps. WET difference maps identified the same regions of under/over-ranging for all patients with large anatomical changes. This was true even for PT#8 and PT#20, in spite of the full magnitude of the over-ranging not being fully recovered due to limitations of the corrected vCT to reproduce complex shrinkage and/or density changes (Fig. 5). In cases of smaller changes or setup variations, the WET difference maps were less uniform. In general, values of $WET_{over-95\%}$ needed to exceed 15mm before significant dosimetric changes could be detected. The most common issues that could lead to a replan were loss of tumor volume coverage, increase in maximum dose to the cord, and over-ranging of dose into the heart.

4. DISCUSSION

In proton therapy, accurate Hounsfield units are a requirement to make clinical decisions for ART. CBCT plays an important role in image-guided therapy, and vCTs is one step in that direction and may play a complementary role to rCT.

In terms of WET information, although the vCT may not reproduce identical WET maps, it identifies the same trends as the rCT regarding the effect of the WET changes. 90% of the fields with $WET_{under-95\%}/WET_{over-95\%}$ larger than 10mm were properly identified as such from the vCT. The dose warping method reproduced similar clinical indicators for patients with considerable changes that may trigger a replan. The most common issue was loss of target coverage of the iCTV. For PT#1, PT#2 and PT#14, the impact to OARs was detected (esophagus, heart/cord and cord respectively). For PT#8, the changes in OAR dose were not properly detected, while for PT#20 an increase in cord dose was incorrectly detected. When smaller changes occurred, differences in OAR dose were also detected (PT#11, PT#12 and PT#16), but some false positives/negatives occurred for loss of target coverage (PT#13, PT#15 and PT#17). Variations in setup can result in overestimation (PT#9) and underestimation (PT#19) of over-ranging, but with minimal dosimetric impact. In general, OAR doses

were maintained within tolerance; however, special care should be given to fields that point towards an OAR, such as lateral oblique fields that may range out at the heart (PT#2, PT#7 and PT#12).

An important conclusion taken from this retrospective investigation was the necessity to evaluate multiple parameters during the ART decision-making process: changes in WET, qualitative review of images and dose distributions, DVHs and corresponding dose-statistics. Flags raised by a single indicator should be backed by additional evidence. For example, iCTV-$V_{99\%}$ statistic was quite sensitive even when the DVHs did not reflect major changes. In cases where the anatomical changes are small the decision to replan should not be based on individual scans, but rather on continued monitoring. Smaller changes can in fact be comparable to setup errors and may average out.

The limitations of the proposed workflow were identified through an evaluation using a diverse cohort of patients. DIR has inherent uncertainties and associated errors, and traditional algorithms are not adequate when tissue appears/disappears (such as atelectasis). If unaccounted for, such situations result in significant errors in WET/range estimation. The correction step works well for gross registration errors, but cannot recover complex changes in tumor topology. When applying the method prospectively and if the correction step is not adequate, manual adjustments to the vCT may be necessary during the second decision-making point (i.e., offline review of vCT). Using CBCT directly for dose recalculation is a viable alternative to remove the errors associated with DIR. Despite the vast work on directly using CBCT in conventional photon therapy[14,30] and/or to improve CBCT image quality[31,32], its usability is still limited in proton therapy[18,33] and therefore the corrected vCT is a good interim solution. For smaller registration errors, we identified two common patterns of failure: first, the interface of lung-tissue-bone at the posterior rib wall due scatter artifacts, and second, the positioning of the scapula (which can often move in and out of the path of lateral oblique fields). From a clinical perspective, two scenarios are possible with DIR errors. The first is a false positive trigger, i.e., the dose calculated on the vCT indicated a change in dosimetry when there is none. The outcome is an unnecessary CT scan to confirm the findings. The other is a false negative trigger, i.e., the dose calculated on the vCT failed to detect the change in dosimetry. While this scenario poses a bigger risk it is unlikely to occur. Higher DIR errors are associated with larger anatomical changes, and in such cases variations in dosimetry are usually still predicted even if with a different magnitude.

The use of CBCT instead of rCT has its own associated challenges. First, subtle changes in density of lung tissues between planning and verification (PT#20) were undetectable on CBCT but apparent on rCT. Second, the limited FoV and artifacts caused by the couch may result in incomplete information of the external contour. This was problematic for some lateral oblique fields (10% of fields); regardless, it can be avoided by closely matching the patient geometry near the beam entrance during

image acquisition. This is not a limitation of the proposed workflow for CBCT systems with larger FoVs.

We established that a vCT is comparable to rCT; the next step is to test the workflow on a larger cohort and transition the workflow to clinical routine. The clinical indicators investigated here were empirically sensible; yet further investigations are required for defining the appropriate action threshold for replanning. On the technical side, improvement of the workflow to minimize its current limitations is a priority, which includes investigating lung-specialized DIR algorithms,[34] automatic segmentation validation,[19] improvement of CBCT image quality[32] and integration with TPS or using more accurate dose calculations.[35]

5. CONCLUSIONS

We retrospectively evaluated a novel workflow to quantitatively assess WET and dose distributions using CBCT for proton therapy. This workflow was shown to provide similar clinical indicators as rCT on patients with considerable interfractional anatomical changes.

FIGURE LEGENDS

Table 1- Patient characteristics.

Figure 1- Workflow for ART. A corrected vCT was created using pCT-to-CBCT DIR, and the variation in WET between vCT and pCT was used to range-correct the planned dose. This process can be performed online to trigger an in-depth offline review of the vCT (and rCT) if deemed necessary.

Figure 2- Images used and generated by the workflow for PT#1 (atelectasis), PT#2 (large tumor shrinkage) and PT#4 (small tumor shrinkage). A consistent soft tissue window level was used for CT datasets (except the CBCT). For PT#1 and PT#2, the vCT needed the correction step (region defined by the red contour). For PT#4, DIR alone recovered the changes well; however, CBCT truncation affected the similarity between vCT and rCT.

Figure 3- Images used and generated by the workflow for PT#3 (lung reinflation), PT#14 (regression of infiltrating tumor) and PT#13 (shrinkage and changes in breathing pattern). A consistent soft tissue window level was used for CT datasets (except the CBCT). For PT#3 and PT#14, correction of the vCT was necessary (region defined by the red contour). For PT#13, DIR was able to recover the tumor shrinkage; however, visible differences in setup occur between vCT and rCT, particularly in the position of the main airways (yellow arrow).

Figure 4- (A) Color overlay of the CTs and corresponding dose distributions and (B) DVHs for PT#1, PT#2 and PT#4. For PT#1 the appearance of atelectasis increased the WET, resulting in under-ranging and loss of iCTV coverage. For PT#2 the shrinkage of the GTV resulted in decreased WET, and thus in over-ranging and increase in dose delivered to the heart and cord. For PT#4 the changes in WET were small in spite of CBCT truncation, resulting in similar dose distributions and DVH curves.

Figure 5- WET and WET difference maps for PT#2 (RPO_1 field), PT#8 (PA field) and PT#19 (RPO field).

REFERENCES

1. Belderbos JSA, Heemsbergen WD, De Jaeger K, et al. Final results of a phase I/II dose escalation trial in non-small-cell lung cancer using three-dimensional conformal radiotherapy. *Int J Radiat Oncol Biol Phys* 2006;66(1):126-134.

2. Machtay M, Bae K, Movsas B, et al. Higher biologically effective dose of radiotherapy is associated with improved outcomes for locally advanced non-small cell lung carcinoma treated with chemoradiation: An analysis of the radiation therapy oncology group. *Int J Radiat Oncol Biol Phys* 2012;82(1):425-434.

3. Rosenzweig KE, Fox JL, Yorke E, et al. Results of a phase I dose-escalation study using three-dimensional conformal radiotherapy in the treatment of inoperable nonsmall cell lung carcinoma. *Cancer* 2005;103(10):2118-2127.

4. Bradley J, Graham MV, Winter K, et al. Toxicity and outcome results of RTOG 9311: A phase I-II dose-escalation study using three-dimensional conformal radiotherapy in patients with inoperable non-small-cell lung carcinoma. *Int J Radiat Oncol Biol Phys* 2005;61(2):318-328.

5. Bradley JD, Moughan J, Graham MV, et al. A phase I/II radiation dose escalation study with concurrent chemotherapy for patients with inoperable stages I to III non-small-cell lung cancer: Phase I results of RTOG 0117. *Int J Radiat Oncol Biol Phys* 2010;77(2):367-372.

6. Levin WP, Kooy H, Loeffler JS, DeLaney TF. Proton beam therapy. *Br J Cancer* 2005;93(8):849-854.

7. Simone CB 2nd, Rengan R. The use of proton therapy in the treatment of lung cancers. *Cancer J* 2014;20(6):427-432.

8. Roelofs E, Engelsman M, Rasch C, et al. Results of a multicentric in silico clinical trial (ROCOCO) comparing radiotherapy with photons and protons for non-small cell lung cancer. *J Thorac Oncol* 2012;7(1):165-176.

9. Simone CB 2nd, Ly D, Dan TD, et al. Comparison of intensity-modulated radiotherapy, adaptive radiotherapy proton radiotherapy, and adaptive proton radiotherapy for treatment of locally advanced head and neck cancer. *Radiother Oncol* 2011;101(3):382.

10. Chang JY, Zhang X, Wang X, et al. Significant reduction of normal tissue dose by proton radiotherapy compared with three-dimensional conformal or intensity-modulated radiation therapy in stage I or stage III non–small-cell lung cancer. *Int J Radiat Oncol Biol Phys* 2006;65(4):1087-1096.

11. Kesarwala AH, Ko CJ, Ning H, Xanthopoulos E, Haglund KE, O'Meara WP, Simone CB 2nd, Rengan R. Intensity-modulated proton therapy for elective nodal irradiation and involved-field radiation in the definitive treatment of locally advanced non-small-cell lung cancer: a dosimetric study. *Clin Lung Cancer* 2015;16(3):237-44.

12. Berman AT, James SS, Rengan R. Proton beam therapy for non-small cell lung cancer: Current clinical evidence and future directions. *Cancers*. 2015;7(3):1178-1190.

13. Wink KCJ, Roelofs E, Solberg T, et al. Particle therapy for non-small cell lung tumors: Where do we stand? A systematic review of the literature. *Front Oncol* 2014;4:292

14. Yang Y, Schreibmann E, Li T, et al. Evaluation of on-board kV cone beam CT (CBCT)-based dose calculation. *Phys Med Biol* 2007;52(3):705.

15. Grills IS, Hugo G, Kestin LL, et al. Image-guided radiotherapy via daily online cone-beam CT substantially reduces margin requirements for stereotactic lung radiotherapy. *Int J Radiat Oncol Biol Phys* 2008;70(4):1045-1056.

16. Landry G, Desdes G, Zollner C, et al. Phantom based evaluation of CT to CBCT image registration for proton therapy dose recalculation. *Phys Med Biol* 2015;60(2):595-613.

17. Landry G, Nijhuis R, Dedes G, et al. Investigating CT to CBCT image registration for head and neck proton therapy as a tool for daily dose recalculation. *Med Phys* 2015;42(3):1354-1366.

18. Veiga C, Alshaikhi J, Amos R, et al. Cone-beam computed tomography and deformable registration-based "dose of the day" calculations for adaptive proton therapy. *Int J Particle Ther* 2015;2(2):404-414.

19. Peroni M, Ciardo D, Spadea MF, et al. Automatic segmentation and online virtual CT in head-and-neck adaptive radiation therapy. *Int J Radiat Oncol Biol Phys* 2012;84:e427–e433.

20. Rit S, Vila Oliva M, Brousmiche S, et al. The Reconstruction Toolkit (RTK), an open-source cone-beam CT reconstruction toolkit based on the Insight Toolkit (ITK). *J Phys: Conf Ser* 2014: 489; 012079.

21. Janssens G, Jacques L, Orban de Xivry J, et al. Diffeomorphic registration of images with variable contrast enhancement. *Int J Biomed Imaging* 2011;2011(Mi):891585.

22. Sonke JJ and Belderbos J. Adaptive radiotherapy for lung cancer. *Semin Radiat Oncol* 2010; 20(2):94-106.

23. Bernard G, Verleysen M, Lee JA. Incremental classification of objects in scenes: Application to the delineation of images. *Neurocomputing* 2015;152:45-57.

24. Cousty J, Bertrand G, Najman L,Couprie M. Watershed cuts: minimum spanning forests and the drop of water principle. *IEEE Trans Pattern Anal Mach Intell* 2009;31(8):1362-1374.

25. Freund Y, Schapire RE. Large margin classification using the Perceptron algorithm. *Machine Learning* 1998;37(3):277-296.

26. Gallant SI. Perceptron-based Learning Algorithms. *IEEE Trans Neural Netw* 1990;1(2):179-191.

27. XXX. The accuracy of deformable registration for adaptive lung proton therapy" Med Phys 2016 *(in review)*.

28. Urie M, Goitein M, Wagner M. Compensating for heterogeneities in proton radiation therapy. *Phys Med Biol* 1984;29(5):553-66.

29. Park PC, Cheung J, Zhu XR, et al. Fast range-corrected proton dose approximation method using prior dose distribution. *Phys Med Biol* 2012;57(11):3555-3569.

30. Guan H, Dong H. Dose calculation accuracy using cone-beam CT (CBCT) for pelvic adaptive radiotherapy. *Phys Med Biol* 2009;54(20):6239–6250.

31. Li J, Yao W, Xiao Y, Yu Y. Feasibility of improving cone-beam CT number consistency using a scatter correction algorithm. *J Appl Clin Med Phys* 2013;14:167-176.

32. Park Y-K, Sharp GC. Phillips J, Winey BA. Proton dose calculation on scatter-corrected CBCT image: feasibility study for adaptive proton therapy. *Med Phys 2015*;42(8):4449-4459.

33. Kurz C, Dedes G, Resch A, et al. Comparing cone-beam CT intensity correction methods for dose recalculation in adaptive intensity-modulated photon and proton therapy for head and neck. *Acta Oncologica* 2015;54:1651-1657.

34. Al-Mayah A, Moseley J, Velec M, Brock K. Toward efficient biomechanical-based deformable image registration of lungs for image-guided radiotherapy. *Phys Med Biol* 2011;56(15):4701-4713.

35. Jia X, Schumman J, Paganetti H, Jiang SB. GPU-based fast Monte Carlo dose calculation for proton therapy. *Phys Med Biol* 2012;57(23):7783-7797.

Table 1- Patient characteristics

PT #	Age (Y)	G	TNM	Fields (gantry angle/name)	V_{iCTV}[a] (cm^3)	F_{rCT}/F_t[b]	Characteristics at verification scan	Tumour motion: SI/LR/AP[c] (mm)	
								pCT	rCT
1	85	M	T3N2M0	175(LPO_1) & 135(LPO_2)	130	9/37	Atelectasis	6/6/4	6/7/5
2	71	F	T3N2M0	210(RPO_1) & 220(RPO_2)	410	20/37	Large tumor shrinkage[d]	8/5/5	10/4/4
3	68	F	T4N2M0	220(RPO) & 180(PA)	280	4/30	Lung reinflation	10/4/10	12/3/2
4	69	M	T4N2M0	180(PA) & 220(RPO)	280	21/37	Small tumor shrinkage/setup error	5/1/3	5/1/3
5	72	M	T3N3M0	180(PA) & 10(RAO)	260	8/27	Tumor position drift	9/2/4	8/3/2
6	81	M	T4N0M0	180(PA) & 155(LPO)	320	9/37	Small tumor shrinkage/setup error	3/1/2	2/1/1
7	77	M	T2aN2M0	180(PA) & 200(RPO)	180	10/37	Small tumor shrinkage/setup error	7/3/2	5/2/2
8	62	F	T4N2M0	270(ASO) & 180(PA)	340	4/34	Large regression of infiltrating tumor	2/3/6	4/2/5
9	64	M	T2aN0M0	180(PA) & 155(LPO)	130	22/37	Small tumor shrinkage/setup error	4/2/2	4/1/3
10	65	M	T4N1M0	180(PA) & 150(LPO)	180	10/25	Small tumor shrinkage/setup error	5/3/4	8/3/4
11	31	M	T2aN2M0	0(AP) & 205(RPO)	200	20/37	Moderate tumor shrinkage[e]	7/2/5	7/4/4
12	76	F	T2bN0M0	180(PA) & 210(RPO)	150	20/37	Moderate tumor shrinkage	2/0/0	2/0/1
13	71	M	T3N2M0	180(PA) & 145(LPO)	190	21/25	Moderate tumor shrinkage	6/3/3	6/3/6
14	65	F	T4N0M0	180(PA) & 150(LPO)	500	20/37	Large regression of infiltrating tumor	2/2/2	1/0/0
15	57	F	T3N2M0	180(PA) & 224(RPO)	340	10/30	Moderate tumor shrinkage	3/2/0	3/3/1
16	58	F	T4N0M0	205(RPO) & 20(LAO)	580	15/33	Moderate tumor enlargement	6/6/4	2/1/1
17	62	F	T1aN2M1b	173(LPO) & 150(LPO)	100	5/37	Moderate tumor shrinkage	2/0/2	3/1/4
18	67	M	T3N1M0	0(AP) & 335(RAO)	330	20/30	Small shrinkage/setup error	3/3/3	5/3/3
19	69	M	T3N0M1b	180(PA) & 205(RPO)	310	7/16	Small shrinkage/setup error	2/2/2	1/1/1
20	78	M	T2aN0M1b	195(RPO) & 210(RPO)	140	9/15	Large tumor shrinkage; density changes	5/2/2	5/4/3

[a] V_{iCTV}=volume of the iCTV

[b] F_{rCT}/F_t=treatment fraction at which rCT was acquired/total number of fractions

[c] SI=superior-inferior; LR=left-right; AP=anterior-posterior

[d] Large tumor shrinkage = visually apparent change in tumor volume greater than 25% of its original GTV.

[e] Moderate tumor shrinkage = visually apparent change in tumor volume less than 25% of its original GTV.

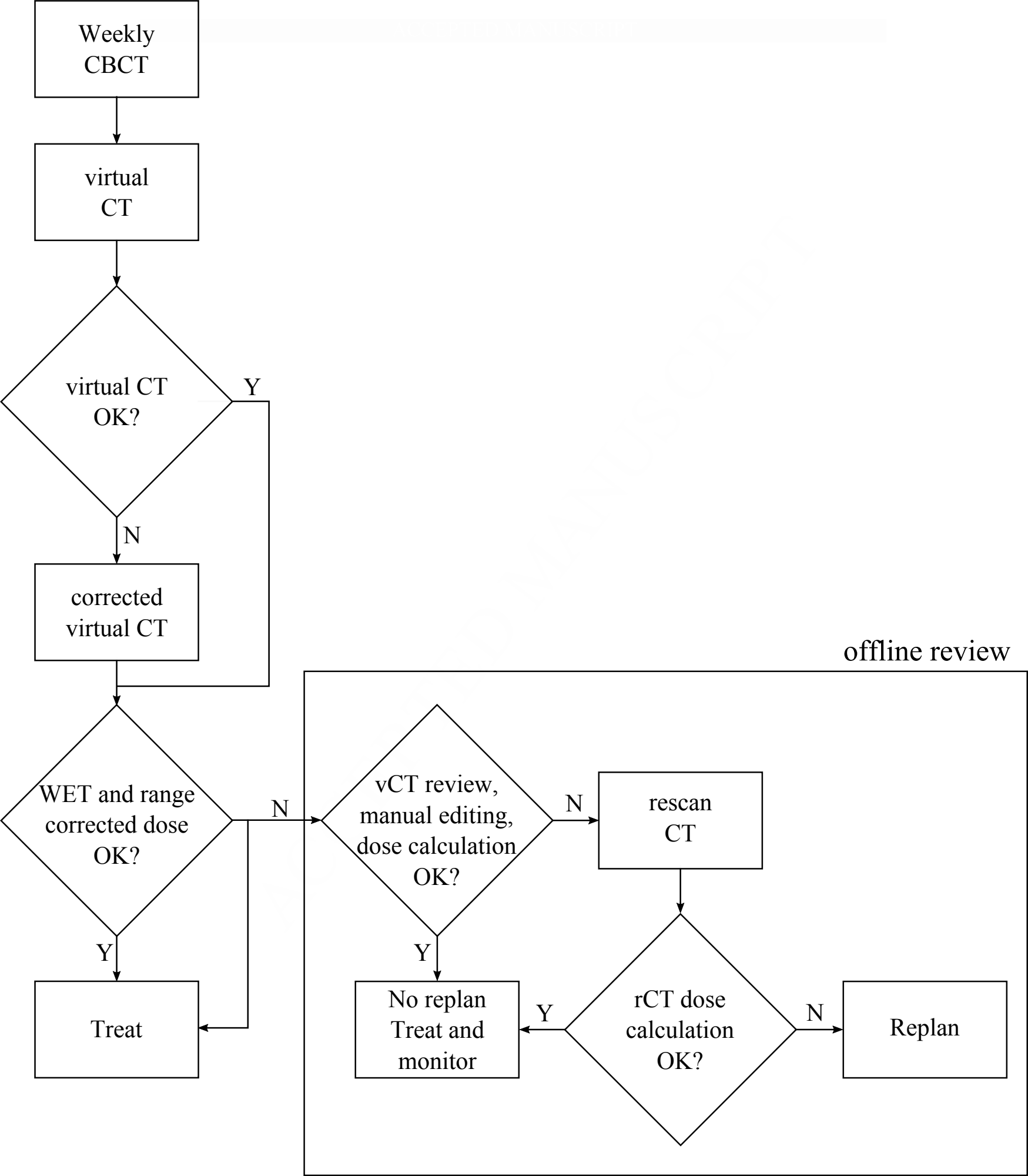
Weekly CBCT
virtual CT
virtual CT OK?
Y
N
corrected virtual CT
WET and range corrected dose OK?
N
Y
Treat
offline review
vCT review, manual editing, dose calculation OK?
N
rescan CT
Y
No replan Treat and monitor
Y
rCT dose calculation OK?
N
Replan

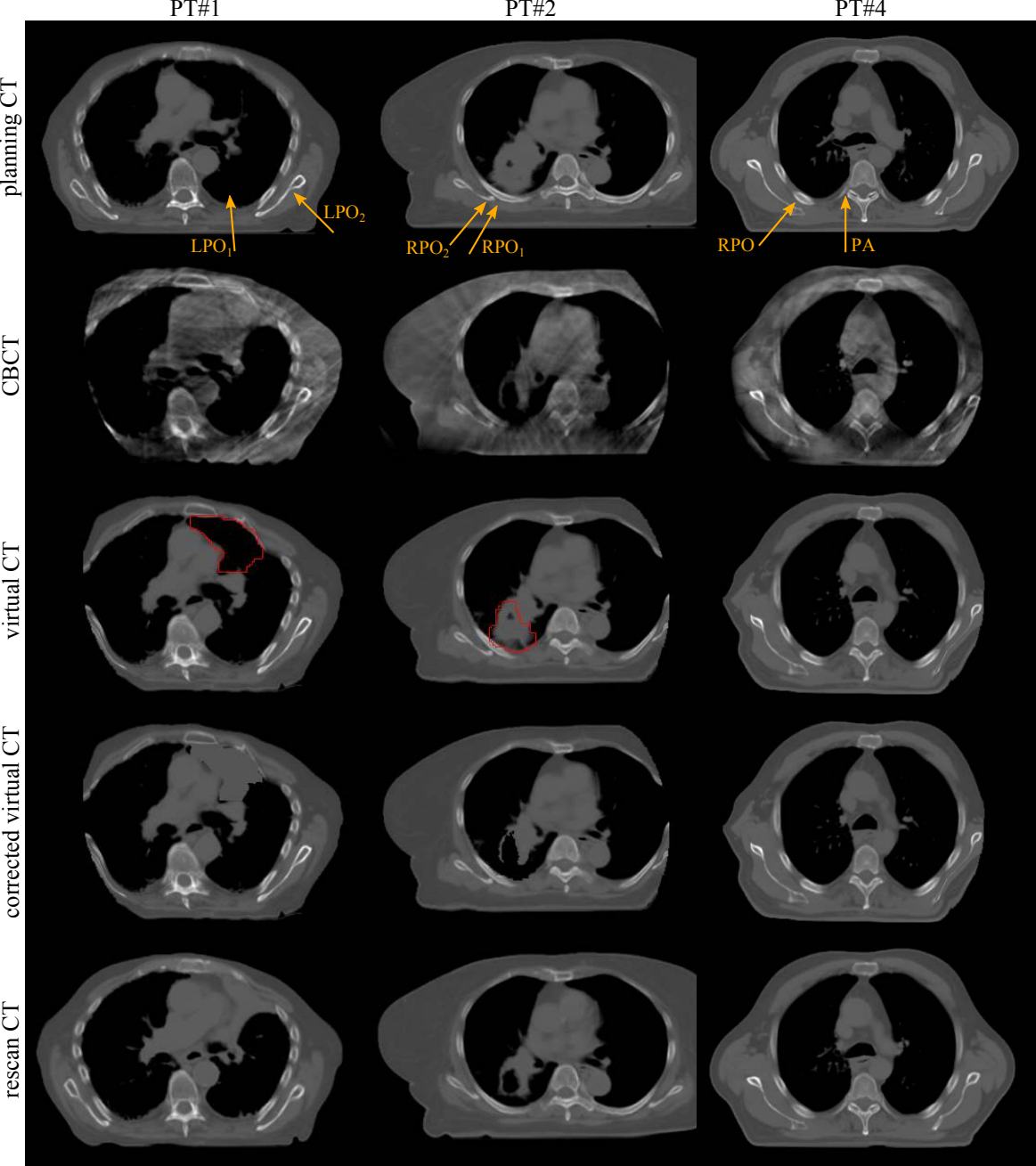
PT#1
PT#2
PT#4
planning CT
CBCT
virtual CT
corrected virtual CT
rescan CT
LPO1
LPO2
RPO2
RPO1
RPO
PA

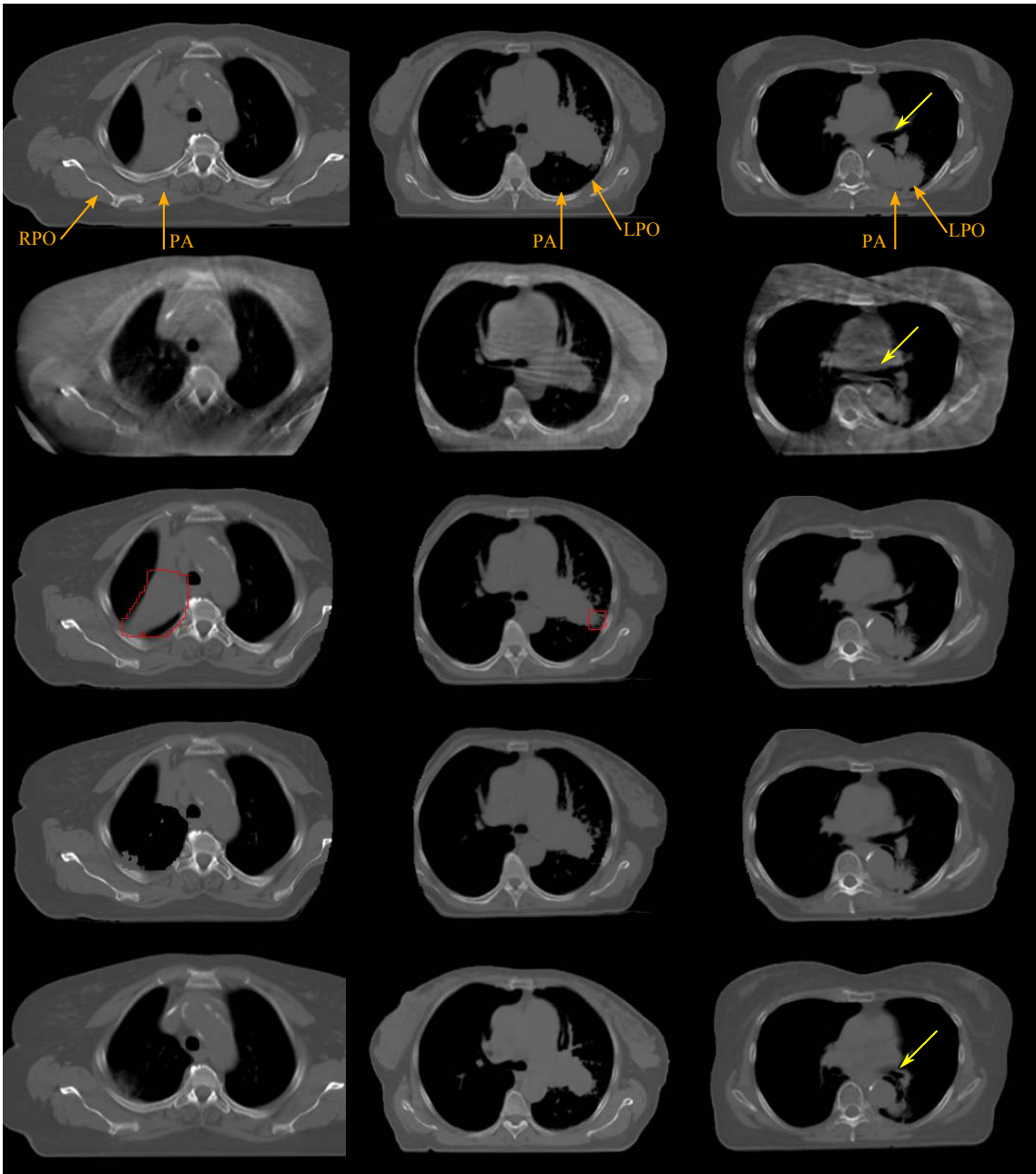
PT#3
PT#14
PT#13
planning CT
CBCT
virtual CT
corrected virtual CT
rescan CT
RPO
PA
PA
LPO
PA
LPO

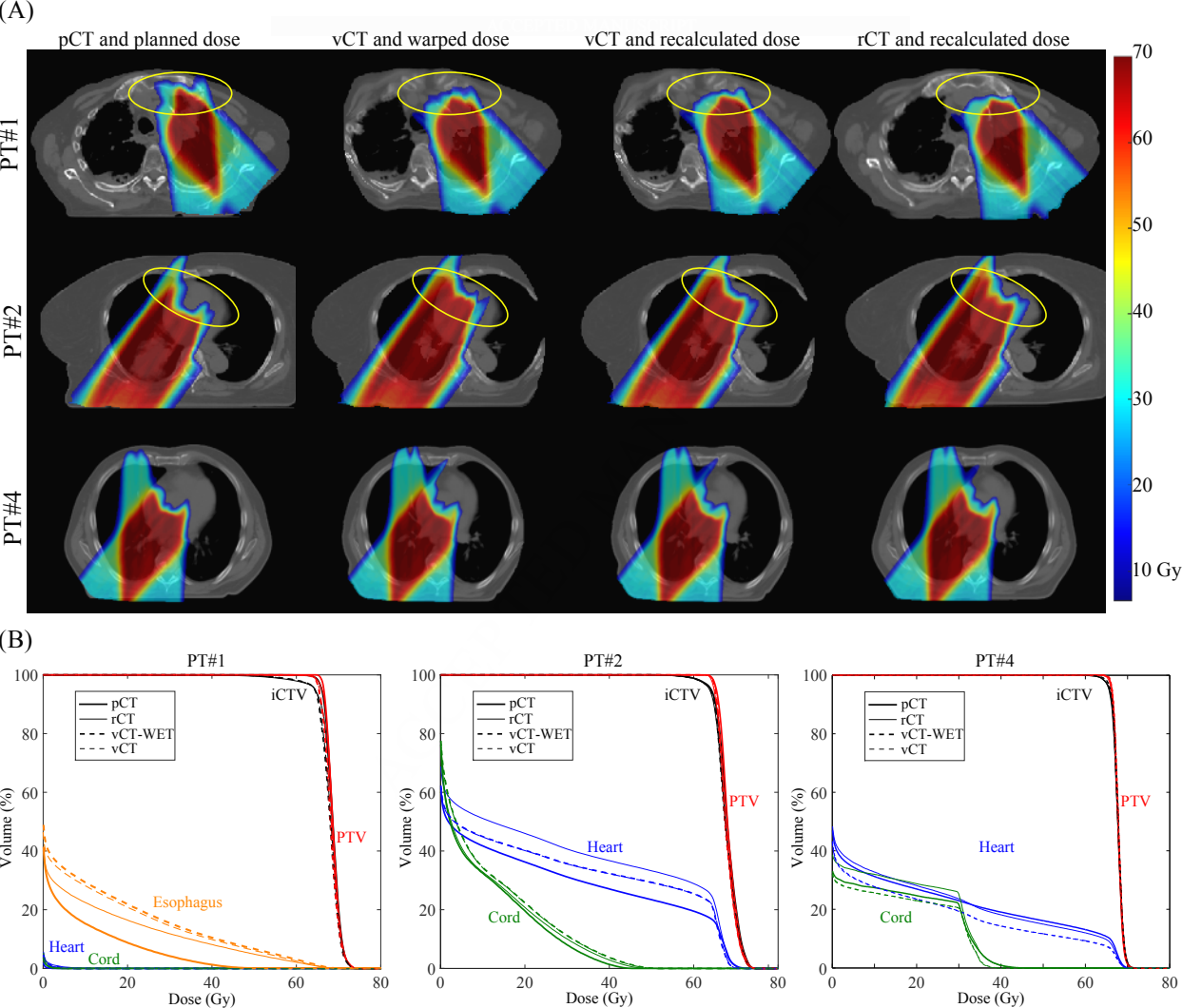
(A)
pCT and planned dose
vCT and warped dose
vCT and recalculated dose
rCT and recalculated dose
PT#1
PT#2
PT#4
70
60
50
40
30
20
10 Gy
(B)
PT#1
PT#2
PT#4
pCT
rCT
vCT-WET
vCT
iCTV
PTV
Esophagus
Heart
Cord
Volume (%)
Dose (Gy)
0
20
40
60
80
100

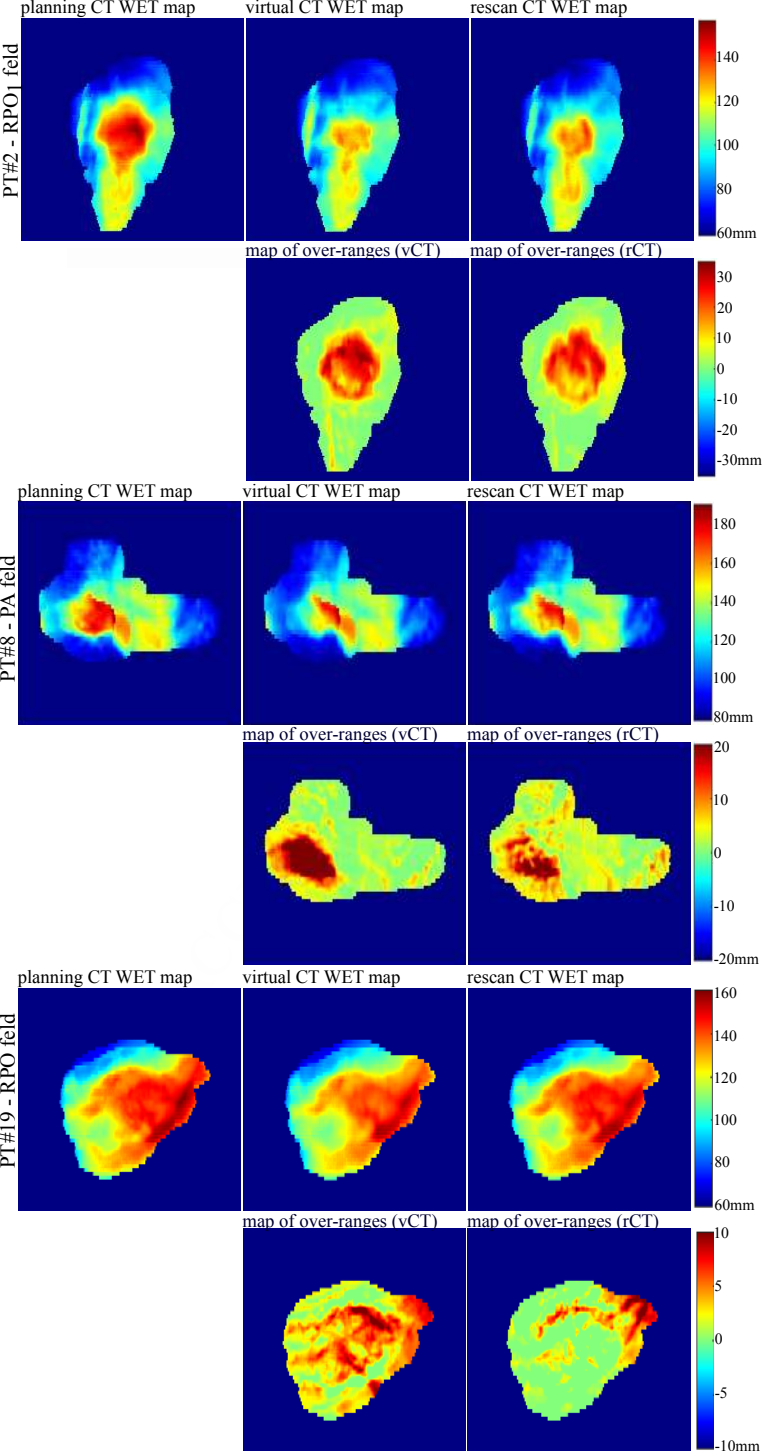
planning CT WET map
virtual CT WET map
rescan CT WET map
PT#2 - RPO1 feld
140
120
100
80
60mm
map of over-ranges (vCT)
map of over-ranges (rCT)
30
20
10
0
-10
-20
-30mm
planning CT WET map
virtual CT WET map
rescan CT WET map
PT#8 - PA feld
180
160
140
120
100
80mm
map of over-ranges (vCT)
map of over-ranges (rCT)
20
10
0
-10
-20mm
planning CT WET map
virtual CT WET map
rescan CT WET map
PT#19 - RPO feld
160
140
120
100
80
60mm
map of over-ranges (vCT)
map of over-ranges (rCT)
10
5
0
-5
-10mm